GEOCHEMICAL BEHAVIOR OF THE SECOND HOT DRY ROCK GEOTHERMAL RESERVOIR AT FENTON HILL, NEW MEXICO

Charles O. Grigsby, P. E. Trujillo, Jr., D. A. Counce, and
R. G. Aguilar

University of California
Los Alamos Scientific Laboratory
Los Alamos, New Mexico

INTRODUCTION

Characteristics of a Hot Dry Rock (HDR) geothermal reservoir were deduced by matching a geochemistry model which incorporates rock dissolution and displacement of an indigenous pore-fluid to chemical analyses of recirculating geothermal fluid. Two reservoirs were created between a pair of wells by hydraulic fracturing. The geometry of these reservoir systems, as well as operational conditions during flow experiments and general heat extraction and water loss performance are described in a preceeding paper by Murphy et al.(1). The first of the reservoirs was evaluated by a 75-day flow test designated as Segment 2. Subsequent operations required the cementing of the injection well to stop a leak behind the casing, and this cementing operation closed the connection to the first reservoir. The second, larger reservoir was evaluated with two flow tests -- the first had a duration of 24 days and is called Segment 4 and the second, called Segment 5, will end on December 19, 1980 after 284 days of operation. Descriptions of the fluid geochemistry in the first reservoir have already been presented by Grigsby and Tester(2), and a preliminary analysis of the Segment 4 test has also been published(3). Present discussion will be mainly concerned with the geochemistry of the second reservoir. Of particular interest in a HDR geothermal reservoir is the relationship between the mixed-mean temperature of the geothermal fluid as measured with a downhole thermistor and the temperatures given by the silica and the Na-K-Ca geochemical thermometers. As will be shown, the temperatures predicted by applying the chemical geothermometers directly to the produced fluid composition at a given time do not represent the true current reservoir temperature.

GEOCHEMISTRY

Fluid samples were analyzed for pH, Eh, conductivity, SiO_2, Na^+, K^+, Ca^{++}, Li^+, B, $SO_4^=$, Cl^-, HCO_3^-, and F^- and samples of the gas dissolved in the liquid were analyzed for H_2, N_2, O_2, CO_2, H_2S and Rn. The data for SiO_2 and Cl^- are plotted vs time for Segments 4 and 5 in Figures 1 and 2 to illustrate the behavior of the system. The rapid decline in both silica and chloride shown in the first eight days in Fig. 1 is due to open-loop operation when the produced fluid was discarded rather than re-injected. After closed-loop operation was established in day 8, the produced fluid is re-injected and the silica and chloride concentrations rapidly attained steady-state levels. The graphs in Fig. 2 also show decline from the high initial concentrations to steady-state levels, however, due to the absence of a long period of open-loop operation in the Segment 5 test, steady-state conditions were reached much more rapidly.

Two types of behavior are discernable from analysis of the fluid chemistry. In the first, the concentration of an aqueous species is fixed by mineral-water equilibria. An example of this is the quartz-water system which fixes the silica concentrations in solution. On the other hand certain species like Cl^- and B, do not result from equilibrium with any known mineral in the rock. The constant ratio of boron to chloride(3) suggests that these species are present in the rock as interstitial salts or pore-fluid. When a flow experiment is initiated in a fracture, some of this pore-fluid is displaced immediately, resulting in the high initial concentrations of Cl^- observed in Figs. 1 and 2. Long-term circulation will eventually sweep the fluid from the rock pores and microcracks that are connected to the main flow system. The dissolved ions in the pore-fluid will maintain a constant ratio in the fluid produced at the surface when the effects of addition of different species concentrations in the make-up water are accounted for. These ratios in the pore-fluid are most easily seen by plotting the nondimensional concentration $\langle C \rangle$ defined as

$$\langle C \rangle \equiv \frac{C^{\infty} - C}{C^{\infty} - C_m}$$

for several dissolved species vs. time where C^{∞} is the concentration of a given species in the pore fluid, C_m is the concentration in the make-up fluid, and C is the concentration of that species in the produced fluid at time t. Plots of $\langle C \rangle$ vs. time for sodium, potassium, chloride, and boron for the Segment 4 test are shown in Fig. 3. Values for C^{∞} for each of these curves are simply the measured concentrations of these species in the earliest samples taken at the production well during the start of a flow experiment. The values for C_m are the measured concentrations in the makeup fluid.

MODELING

It was found from the results of the Segment 2 test(4) that the geochemical behavior of the early system could be adequately described by two parallel flow paths at different temperatures. Such a model is shown schematically in Fig. 4. The changes in concentration of a chemical species resulting from mineral dissolution or pore-fluid displacement in both flow paths are derived by writing a mass balance on each species and on the total mass in the system. Many of the terms used in the model to account for the rate of dissolution or displacement in the separate flow paths are not directly measurable; therefore, the unknown parameters are lumped into two temperature dependent parameters. These parameters are adjusted within reasonable limits to match the actual behavior measured under open- or closed-loop experimental conditions. Comparisons of the best-fit solutions obtained for the data from Segment 4 are shown in Fig. 5. The close fit of the calculations with the actual data suggests that a simple model with two parallel paths is sufficient at the present time to describe pore-fluid displacement in the reservoir.

GEOTHERMOMETRY

If two parallel flow paths at different temperatures and residence times are conducting fluid through the reservoir, the produced fluid compositions will result from the combination of reaction rates, residence times and flow rates in each of the flow paths. Estimates of the flow split between the paths can be made by considering a species such as Cl^- which does not result from mineral-water reactions in the reservoir. From the closed-loop portion of the Segment 4 test, ∼92.5% of the fluid passes through the main fracture system while the other 7.5% passes through the secondary path. Because there will be insignificant thermal drawdown and long contact times between fluid and rock, the fluid passing through this secondary flow path will truly reflect the mean rock temperature in this path. The quartz geothermometer(5) and the Na-K-Ca geothermometer(6) temperatures have been calculated for the fluid produced during Segments 4 and 5. Graphs of these temperatures as well as the downhole measured temperatures are shown in Fig. 6. Since no thermal drawdown was measured in the Segment 4 test, it is not surprising that no decline in geothermometer temperature is seen in Fig. 6a. There is, however, measurable decline in downhole temperature in the Segment 5 test. This temperature decline is observed in the quartz geothermometer; however, no similar decline is seen in the Na-K-Ca geothermometer. In addition, the Na-K-Ca geothermometer is affected significantly less during the open-loop portion of Segment 4 than is the quartz geothermometer. This insensitivity of the Na-K-Ca geothermometer to reservoir temperature decline and to changes in inlet fluid composition during a test is due to the constant Na/K ratio in the pore-fluid which is displaced from the secondary flow path. This Na/K ratio is fixed by equilibrium with the feldspars at the initial rock temperature (∼190°C) and dilution of the pore-fluid with fresh water does not affect the Na/K ratio in the produced fluid. Because re-equilibration of this geothermometer is extremely slow (see, for example, ref 7) the Na-K-Ca geothermometer reflects the initial rock temperature rather than changes in the reservoir temperature due to heat extraction.

The quartz geothermometer, on the other hand, is affected by changes in temperature in the main flow path as well as changes in the inlet fluid composition. This is seen in the first eight days of the Segment 4 test (Fig. 6a) as well as in three periods of open-loop circulation at about days 102, 110 and 230 in the Segment 5 test (Fig. 6b). The sudden change in inlet fluid composition in the Segment 5 test exceeded the ability of the main flow path to dissolve quartz and thus raise the silica concentration in the produced fluid. Re-establishing the closed-loop mode resulted in a rapid rise in the silica concentration back to the pre-open-loop levels. Interpretation of this response and of the application of the quartz geothermometer to the HDR system are in progress, however, incomplete knowledge of the temperature dependence of the rate of dissolution of quartz has hampered further development of the analysis.

CONCLUSIONS

The results of three major heat-extraction experiments conducted in two hot dry rock geothermal reservoirs indicate that the fluid chemistry is largely influenced by the interstitial fluid contained in the reservoir rock. This fluid is slowly removed by the circulation of relatively fresh water through the fracture systems until the level of dissolved species is ultimately fixed by rock-water equilibrium. Because the sodium and potassium observed in the system were contributed by the pore-fluid, the Na-K-Ca geothermometer was insensitive to changes in the rock temperatures. The quartz geothermometer does reflect the changes in reservoir temperature, however the concentration of silica in solution must be adjusted for the effect of mixing of small amounts of silica-saturated pore-fluid with fluid which has passed through the main flow path. When the pore-fluid contribution is subtracted, the resulting concentration of silica in the produced fluid can be modeled with a kinetic model to determine the actual temperature of the reservoir rock.

REFERENCES

1. Murphy, H.D., J.W. Tester and R.M. Potter, "Comparison of Two Hot Dry Rock Geothermal Reservoirs," proceedings of 6th Workshop on Geothermal Reservoir Engineering, Stanford, CA, I.G. Donaldson, P. Kruger, and H.J. Ramey, Jr., eds., Dec. 1980.

2. Grigsby, C.O. and J.W. Tester, "Evaluation of the Fenton Hill Hot Dry Rock Geothermal Reservoir, Part II. Flow Characteristics and Geochemistry," proceedings of the Fourth Workshop on Geothermal Reservoir Engineering, Stanford, CA, P. Kruger and H.J. Ramey, Jr., eds., Dec. 1978.

3. Murphy, H.D., ed., Preliminary Evaluation of the Second Hot Dry Rock Geothermal Energy Reservoir: Results of Phase I, Run Segment 4, Los Alamos Scientific Laboratory report LA-8354-MS, 1980.

4. Grigsby, C.O., J. Abbott, L.A. Blatz, C.E. Holley, and J.W. Tester, "Fluid Geochemistry" in Hot Dry Rock Energy Extraction Field Test: 75 Days of Operation of a Prototype Reservoir at Fenton Hill, Los Alamos Scientific Laboratory report LA-7771-MS, J.W. Tester and J.N. Albright, eds., 1979.

5. Morey, G.W., R.O. Fournier, and J.J. Rowe, "The Solubility of Quartz in Water in the Temperature Interval from 250°C to 300°C," Geochim. Cosmochem. Acta 26, 1029-1043, 1962.

6. Fournier, R.O. and A. H. Truesdell, "Chemical Indicators of Subsurface Temperature, Part 2: Estimation of Temperature and Fraction of Hot Water Mixed with Cold Water," J. Res. U.S. Geol. Surv. 2, 263-270, 1974.

7. Charles, R.W., "Experimental Geothermal Loop II, 200°C Study," Los Alamos Scientific Laboratory report LA-7735-MS, April 1979.

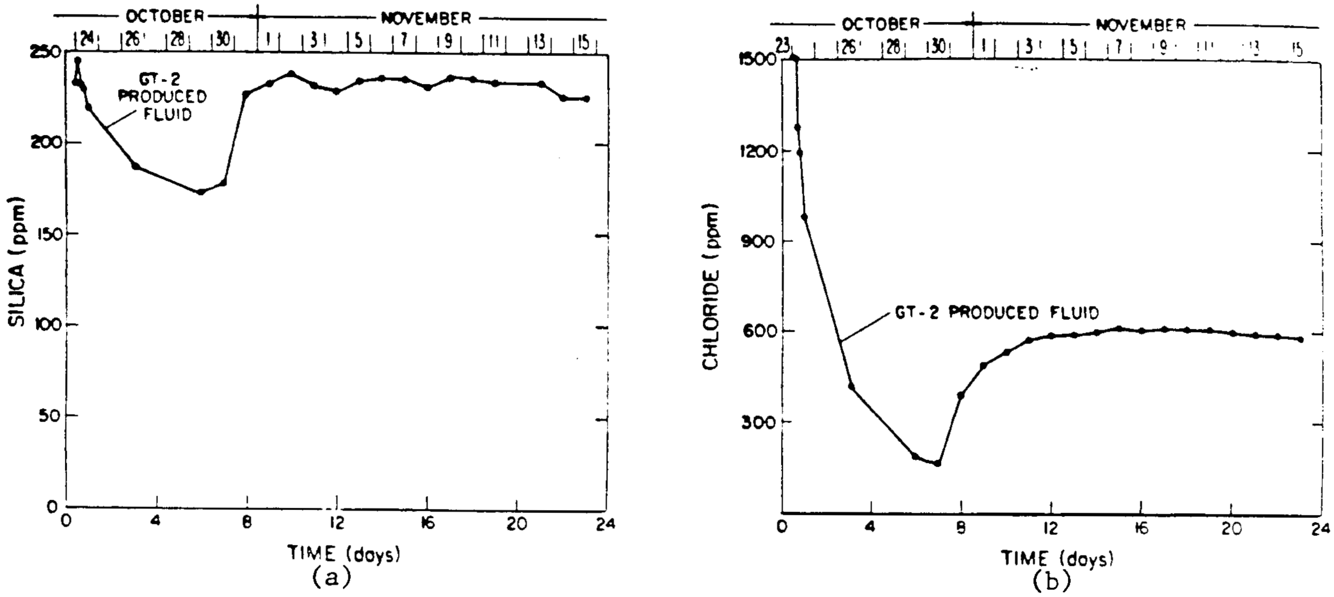

(a) (b)

Figure 1 Silica (a) and chloride (b) variations with time in the Segment 4 test.

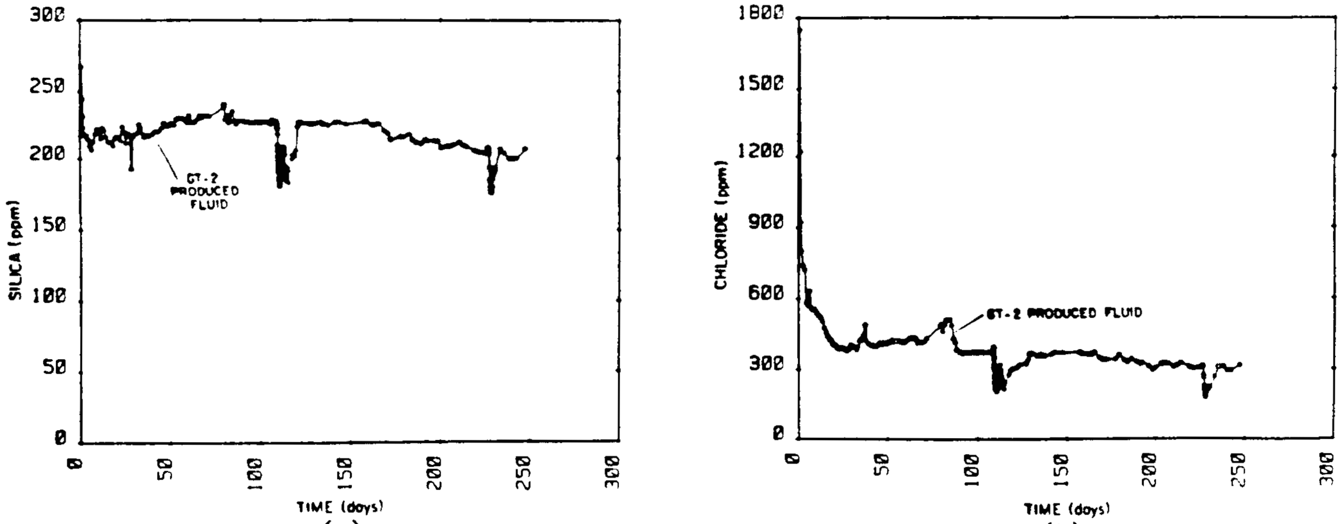

(a) (b)

Figure 2 Silica (a) and chloride (b) variations with time in the Segment 5 test.

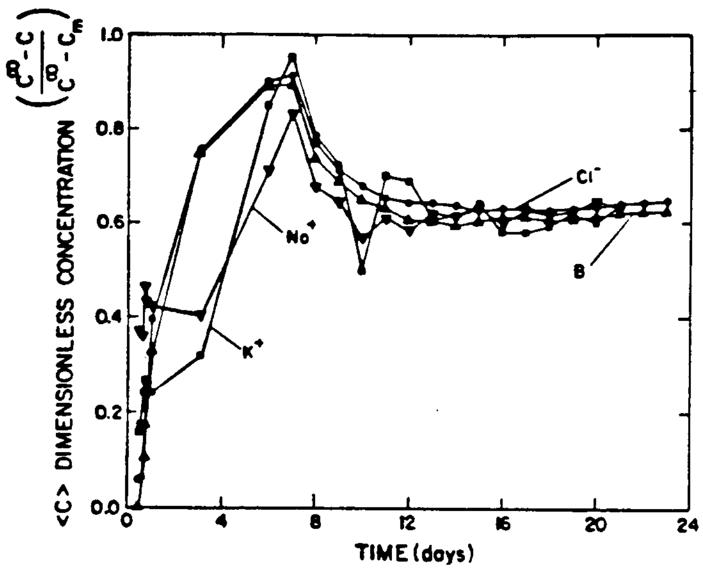

Figure 3 Nondimensional concentrations of Na^+, K^+, Cl^- and B in the produced fluid from the Segment 4 test.

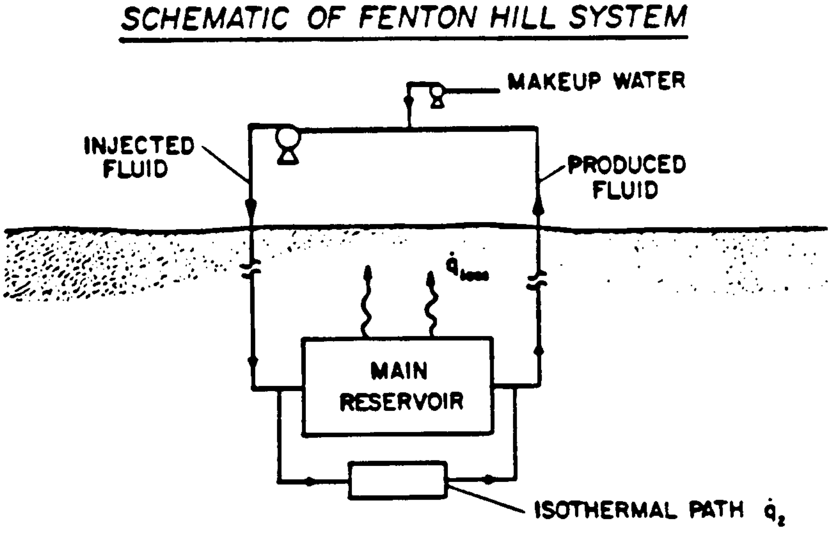

Figure 4 Schematic of the parallel-path model for the Fenton Hill System. The main reservoir consists of the short-residence time fracture system while the isothermal or secondary path has a long residence time.

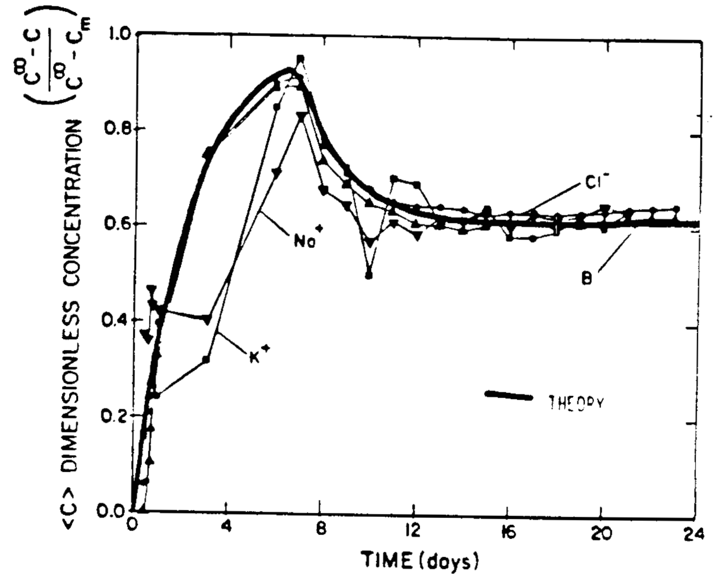

Figure 5 Theoretical fit to the experimental data for the pore-fluid displacement model.

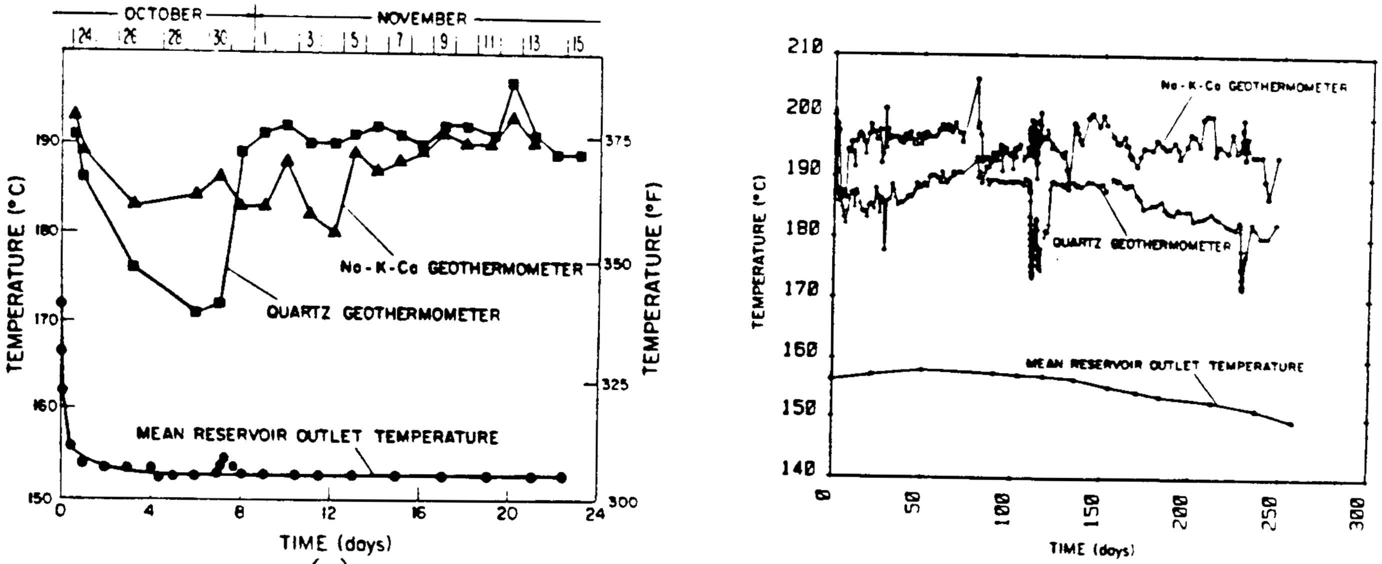

(a)

(b)

Figure 6 Comparison of the Na-K-Ca geothermometer and quartz geothermometer temperatures to the measured downhole reservoir outlet temperature for Segment 4 (a) and Segment 5 (b).